Functionalization of silicone rubber for the covalent immobilization of fibronectin

N. VÖLCKER[1], D. KLEE[1], H. HÖCKER[1], S. LANGEFELD[2]
[1]*Department of Textile and Macromolecular Chemistry, Technical University of Aachen, Veltmanplatz 8, D-52062 Aachen, Germany*
[2]*Department of Ophthalmology at the Technical University of Aachen, Pauwelsstr. 30, D-52057 Aachen, Germany*
E-mail: voelcker@scripps.edu

Surface modification techniques were employed in order to provide functionalized silicone rubber with enhanced cytocompatibility. Acrylic acid (AAc), methacrylic acid (MAAc) and glycidylmethacrylate (GMA) were graft-co-polymerized onto the surface of silicone induced by an argon plasma and thermal initiation. The polymerizations were carried out in solution, in the case of acrylic acid a vapor phase graft-co-polymerization subsequent to argon plasma activation was carried out as well. Human fibronectin (hFn), which acts as a cell adhesion mediator for fibroblasts, was immobilized by making use of the generated carboxylic or epoxy groups, respectively. Surface analysis was accomplished by means of X-ray photoelectron spectroscopy (XPS), infrared spectroscopy in attenuated total reflection mode (IR-ATR), scanning electron microscopy (SEM), atomic force microscopy (AFM) and dynamic contact angle measurements using the Wilhelmy-plate method. The amount of immobilized active hFn was semiquantified by enzyme-linked immunosorbent assay (ELISA) using a structure-specific antibody against the cell-binding domain of hFn. *In vitro* testing showed a remarkable difference between surfaces exposing adsorbed-only and surfaces with covalently immobilized hFn.
© *2001 Kluwer Academic Publishers*

1. Introduction

For more than two decades, silicone rubber has been used in ophthalmology, e.g., as contact lenses, intraocular lenses or artificial orbita [1]. Recently, an artificial cornea and a retinal patch containing parts out of silicone were described [2, 3]. Due to its mechanical and optical properties, it is still the material of choice for an increasing number of implants [4]. As far as transparency and oxygen permeability are concerned, no other polymer matches up to this material [5, 6].

Though, for many biomedical applications, silicone has still not achieved commercial success. Due to the fact that its chemical nature as well as its hydrophobicity prevent cells at the implantation site from adhering but also lachrymal liquid from moisturing, this repulse ought not to be surprising [7].

The need to improve the biocompatibility of silicone brings up attempts to modify its surface while leaving bulk characteristics unchanged. Surface modifications have been performed by plasma etching [8], radiation grafting, plasma-induced graft-co-polymerization [9], photo-chemical grafting and plasma polymerization [10, 11]. Monomers like 2-hydroxyethyl methacrylate (HEMA) have been used frequently in order to form a hydrogel layer [12, 13]. Apart from functionalization, it is desirable to use bifunctional moieties as spacer molecules for the subsequent attachment of bioactive species. In this context, isocyanates, aldehydes, carboxylic and epoxy functional groups are commonly employed [14–16]. In order to enhance cell growth on the material, cell adhesion mediators like fibronectin, laminin or vitronectin are subjected to adsorption on various surfaces [17, 18]. Covalent immobilization of proteins on surfaces is considered to bring up a higher bioactivity of the surface in comparison with adsorptively bound protein [19].

The present study involves graft-co-polymerization of AAc, MAAc and GMA on plasma-treated silicone aiming at the generation of a hydrophilic layer on the silicone surface providing the respective functionality. Scheme 1 shows a schematic illustration of the surface modifications by graft-co-polymerization. The introduced reactive species should be used to covalently attach hFn while maintaining its bioactivity as a cell adhesion mediator. Generated carboxylic groups need to be activated prior to hFn immobilization by means of N-ethyl-N′(3-dimethylaminopropyl) carbodiimid hydrochloride (EDC) [20]. Coupling to epoxy groups was accomplished without further activation. The aim of this study was to show a potential application of the surface-modified silicone rubber as an all silicone keratoprosthesis.

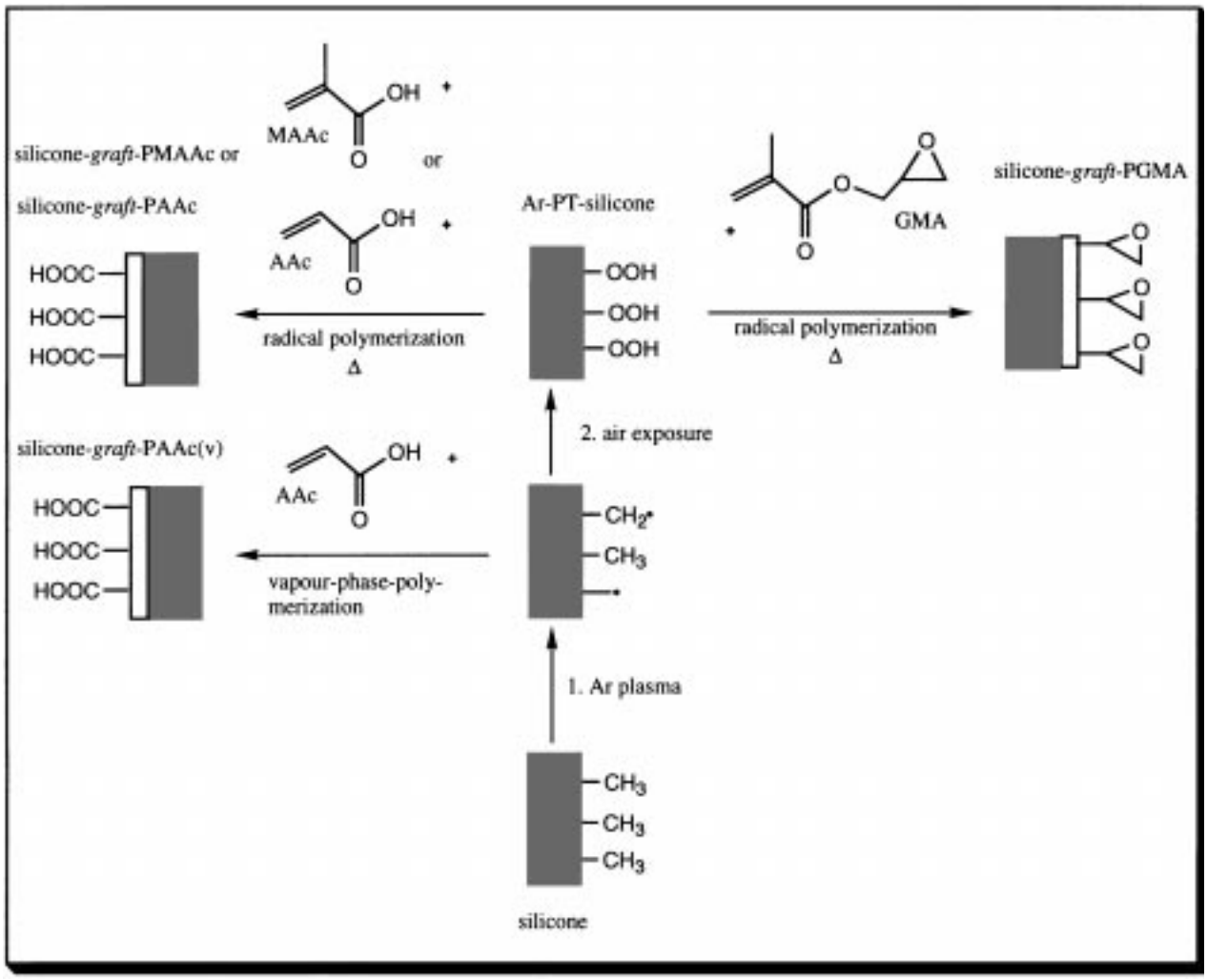

Scheme 1 Sequence of the applied surface modification procedure involving argon plasma treatment and subsequent grafting of monomers.

2. Materials and methods

2.1. Polymer and chemicals

A two silicone elastomer kit (Dow Corning, Sylgard 184, Wiesbaden, Germany) was vulcanized after mixing of the components and degassing at 180 °C for 20 min. Acrylic acid (Fluka, Neu-Ulm, Germany), methacrylic acid (Merck, Darmstadt, Germany) and glycidyl methacrylate (Fluka) were distilled in nitrogen atmosphere in order to remove inhibitors. AAc and MAAc were polymerized in a 20% (v/v) solution of bidistilled degassed water. The material was Soxhlet-extracted with water. GMA was polymerized in a 20% (v/v) solution of degassed cyclohexanone followed by Soxhlet-extraction with 1, 4-dioxane.

2.2. Chemical functionalization

Plasma treatment was performed in a microwave plasma (HEXAGON prototype, *Technics Plasma*). Argon served as the plasma gas. The reactor was evacuated to 5×10^{-5} mbar. After flooding with argon, the pressure was set to 2.2×10^{-1} mbar and plasma ignition was performed in a microwave reactor at 2.45 GHz and 300 W for 60 s. Samples were subsequently exposed to air for 30 min and introduced into the monomer solution. The solution was heated to 90 °C for 2 h. After Soxhlet-extraction, samples were stored in water. Vapor phase graft-co-polymerization of AAc was carried out in an HF-plasma reactor (27.12 MHz, 100 W). Samples were stored in water.

2.3. Chemical characterization

Chemical changes of the silicone surfaces were characterized after each modification step by infra-red spectroscopy in attenuated total reflection mode (IR-ATR) (60 SXR, Nicolet, Offenbach, Germany) (reflection unit: Germanium crystal), X-ray photoelectron spectroscopy (XPS) (SSI 206X/Probe, Surface Science Instruments, Mountain View, CA, U.S.A.) (Al - $K_{\alpha 1,2}$) and contact angle measurements using the Wilhelmy-plate method (Lemke & Partner KW-2P, Kaart, Germany).

2.4. Morphological characterization

In order to investigate changes in surface morphology, scanning electron microscopy (SEM) (Leica S 360, Wetzlar, Germany) was carried out after sputtering with gold (Edwards S 150B). Atomic force microscopy (AFM) (Nanoscope III, Digital Instruments, Santa Barbara, CA, U.S.A.) in contact mode was applied to obtain more detailed topological information.

2.5. Protein immobilization and characterization

Carboxylic groups at the surfaces were reacted with EDC in 0.03 M NaH_2PO_4 buffer (pH 4.8) (0.5 mg/ml) for 30 min at room temperature. After rinsing with NaH_2PO_4 buffer and carbonate/bicarbonate coating buffer (BupH 9.6, Pierce Europe), samples were incubated with 10 µg/ml hFn in BupH 9.6 for 2 h followed by washing with the same buffer.

Epoxy groups at the surfaces were directly incubated with 10 µg/ml hFn in BupH for 2 h followed by washing with the same buffer.

The enzyme-linked immunosorbent assay (ELISA) was carried out according to the following procedure.

6-Well TCPS-clusters were blocked with blocking buffer (4.5 g BSA in 500 ml PBS). After washing with washing buffer (5 ml Tween 20, 1.1 g BSA, 11 PBS) samples were fixated with double-sided adhesive. Protein immobilization followed as described above. The first antibody (mouse-anti-human fibronectin-Fn12-8, monoclonal structure specific antibody against the cell-binding domain) was added in a dilution of 1 : 1250 for 1 h. After washing, the second antibody (rabbit-anti-mouse-IGG (H + L), conjugated to horseradish peroxidase (HRP)) was added in a dilution of 1 : 1250 for 2 h. After washing, the cavities were filled with diammonium-2,2′-azino-di-(3-ethylbenzothiazolin sulfonate) (ABTS) as a substrate in solution with H_2O_2 (1-step® ABTS, Pierce Europe, St. Augustin, Germany) and incubated for 20 min. Optical density of the resulting solution was measured in an ELISA-reader (Spectra, SLT, Crailsheim, Germany) at 405 nm.

2.6. Cell culture

Cell culture experiments were carried out with L929 mouse fibroblasts. Cells were maintained in the following culture medium: RPMI-1640 (Life Technologies, Eggenstein-Leopoldshafeu, Germany) and 10 fetal calf serum (Gibco, Paisley, Scotland) 9 : 1, containing glutamine and penicillin/streptomycin. The cultures were incubated at 37 °C with 7.5% CO_2. Samples in direct contact were fixated to glass slides with a biocompatible adhesive, brought into tissue culture vials and incubated with L929 cells (8×10^5 cells ml^{-1}) for 24 h at 37 °C. Samples in indirect contact (surface area: 30 cm^2) were incubated in 15 ml medium at 37 °C for 24 h. For vital fluorescence staining fluorescein diacetate (FDA) and ethidium bromide (EB) was used. The cell morphology was visualized by hemalaun staining whereas cell viability in indirect contact was assessed as well using the 3-(4,5-dimethylthiazol-2-yl)-2,5-diphenyltetrazolium bromide (MTT) assay [21].

3. Results and discussion

3.1. Characterization of the functionalized silicone surface

In this study, various methods for the functionalization of silicone rubber are suggested (Scheme 1). As a first step the surface of silicone was treated with an argon plasma. The plasma-treated samples were generally exposed to air in order to generate hydroperoxides. In a following step AAc, MAAc and GMA were graft-co-polymerized in solution by thermal initiation. A second pathway was taken in the case of AAc. Argon plasma-treated samples were directly exposed to AAc vapor in order to initiate graft-co-polymerization.

The grafting of AAc and MAAc cannot be detected by IR-ATR whereas grafting of GMA is detectable within the given information depth of 0.1–1 µm. Fig. 1 shows the IR-spectra of silicone rubber, silicone-*graft*-PGMA and PGMA homopolymer. Absorption bands in the spectrum of unmodified silicone can be attributed to Si-CH_3 at 1258 cm^{-1}, Si-O-Si at 1018 cm^{-1} and H_3C-Si-CH_3 at 796 cm^{-1}. These bands are absent in the spectrum of silicone-*graft*-PGMA (b). Only the characteristic bands appearing in the spectrum of PGMA (c) are found, i.e., at 3001–2950 cm^{-1} (C-H stretch), 1727 cm^{-1} (C═O stretch), 1152 cm^{-1} (C-O stretch) and at 907 cm^{-1} (oxirane ring out-of-plane deformation). Apparently, the monomer GMA forms either a thick layer on the surface or penetrates into the silicone bulk. Further information has to be taken from XPS examinations.

The difference in grafting thickness for GMA and the water-soluble acid monomers might result from the fact that silicone rubber does not swell in water, which is used as a solvent for the polymerization of AAc and MAAc. In

TABLE I Untreated and modified silicones characterized by means of XPS for elemental composition, binding energy and ratios of carbon (C1s) and oxygen (O1s) species

Surface	Carbon (C1s)				Oxygen (O1s)				silicon (Si2p)
	total atom-%	285.0 eV	286.9 eV	289.2 eV	total atom-%	532.6 eV	533.1 eV	533.8 eV	
		C-H, C-C, C-Si	C-O	O-C═O		O═O, O-Si	O-C═O	C-O-C	total atom-%
Silicone untreated	47.4	47.4%			25.1	25.1%			27.5
Ar-PT-silicone	39.0	33.2%	5.8%		31.6	31.6%			29.2
Silicone-*graft*-PMAAC	50.2	43.9%	4.2%	2.1%	26.3	22.2%		4.1%	22.4
PMAAc	77.6	62.3%	6.5%	8.8%	20.4	11.9%		8.5%	2.0
Silicone-*graft*-PAAc	52.4	47.7%	2.7%	2.0%	25.1	22.1%		3.0%	22.3
Silicone-*graft*-PAAc(v)	53.3	43.6%	4.7%	5.0%	30.1	24.3%		5.8%	16.6
PAAc	78.5	63.3%	4.9%	10.4%	19.3	12.2%		7.1%	1.2
Silicone-*graft*-PGMA	64.1	38.1%	19.2%	6.8%	25.9	19.8%		6.1%	10.0
PGMA	74.2	48.6%	19.8%	5.8%	22.1	15.7%		6.4%	3.7

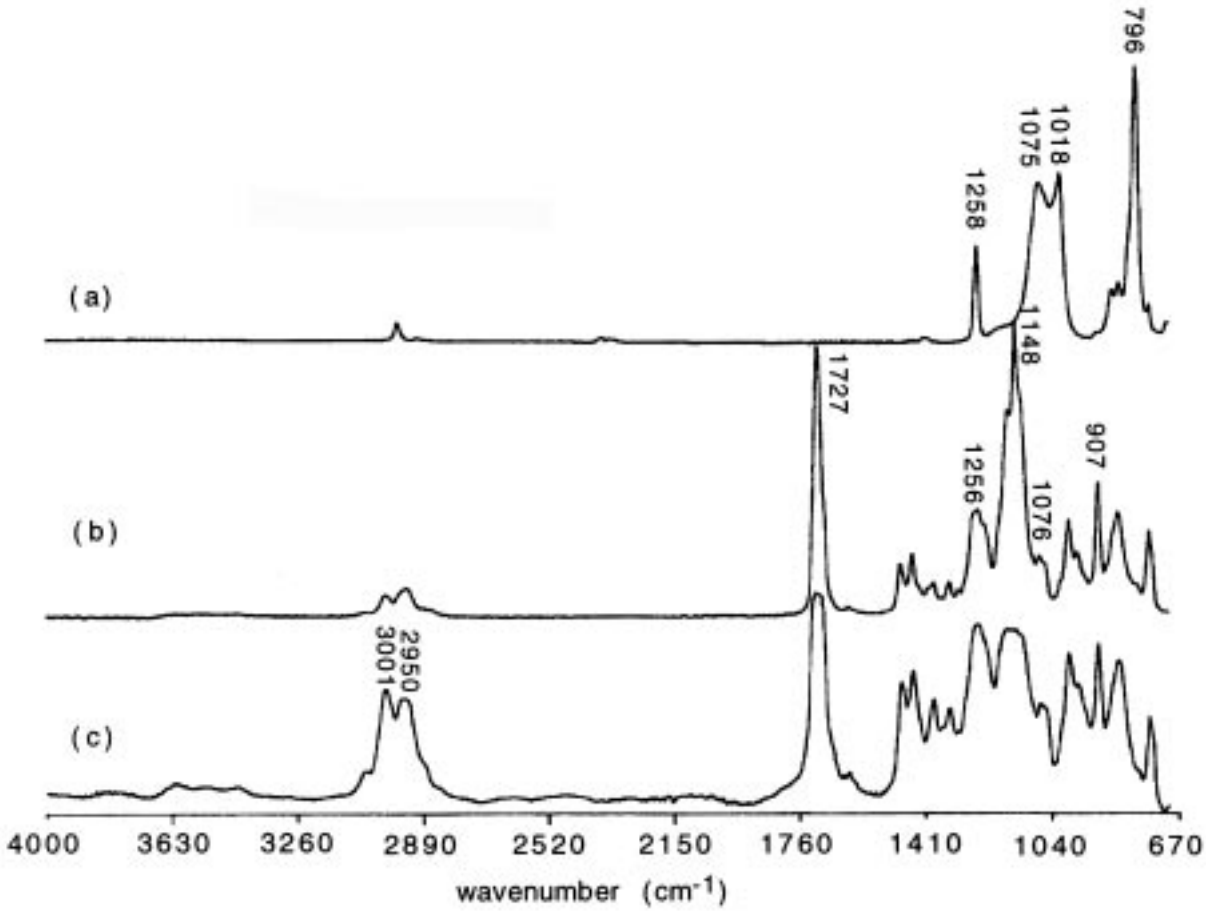

Figure 1 Overlay of IR-ATR spectra: (1) unmodified silicone; (2) silicone-*graft*-PGMA; (3) PGMA.

contrast, GMA is graft-co-polymerized in cyclohexanone, which is able to swell the bulk polymer.

XPS data showing the elemental composition as well as the different carbon and oxygen species are listed in Table I.

Argon plasma treatment (Ar-PT-silicone) leads to an increase in oxygen content (31.6 atom-%) and to a decrease in carbon. After deconvolution of the C1s spectrum, an additional peak appears at a binding energy of 286.5 eV which is assigned to C-O carbon.

In comparison with the results of IR-ATR, XPS reveals surface changes upon graft-co-polymerization of AAc. In Fig. 2 C1s spectra of two different PAAc grafted surfaces are shown. The silicone-*graft*-PAAc (b) is obtained by solution grafting. Surface (c), which refers to silicone-*graft*-PAAc(v) is produced by vapor phase graft-co-polymerization. In both spectra the presence of oxidized carbon species is obvious. Carboxylic groups are indicated by the peak of O-C=O carbon at 289.2 eV which also appears in the C1s spectrum of PAAc (d). The surface (c) shows 5.0 atom-% carboxylic groups, whereas surface (b) shows only 2.0 atom-%. After deconvolution a peak at 286.5 eV becomes evident for surface (b) and (c) and also for the homopolymer surface (d). It can be assigned to side products formed during polymerization.

In the deconvoluted data of the O1s spectra (Table I) a higher oxygen amount is detected for vapor phase grafted PAAc than for solution grafted PAAc. This goes along with a lower silicon content (16.6 atom-%) for silicone-*graft*-PAAc(v) compared to 22.2 atom-% for silicone-*graft*-PAAc. The oxygen position of O=C groups at 532.6 eV overlaps with the siloxane signals, whereas the peak at 533.8 eV is attributed exclusively to O-C=O oxygen of carboxylic groups. This peak is therefore an indicator for the percentage of AAc present on the surface as seen by XPS. Surface (c) shows an O-C oxygen content of 5.8 atom-%, whereas (b) shows only 3.0 atom-%. The same difference of about 3 atom-% is observed for the intensities of the O-C=O C1s peak at 289.2 eV for surfaces (b) and (c).

According to Table I, XPS results very similar to those for surface (b) are obtained for silicone-*graft*-PMAAc. 2.1 atom-% of O–C=O carbon and 43.9 atom-% of C-C/C-H carbon at 285.0 eV are present on the surface. 4.1 atom-% of O-C oxygen are detected.

A residual silicon content of about 22 atom-% is measured for the surfaces of silicone-*graft*-PAAc and silicone-*graft*-PMAAc. The grafted layer seems to be thinner than the information depth of 10 nm. Other authors point out that grafting of hydrogels on polymers with low glass temperature leads to migration effects in order to reduce the interfacial free energy [22, 23]. Consequently, the surface presented to air or vacuum might be significantly different from that presented to hydrophilic ambience like water.

Fig. 3 shows the C1s peaks of unmodified silicone (e) in comparison with silicone-*graft*-PGMA (f) and PGMA homopolymer (g). Surfaces (f) and (g) show similiar C1s contributions. Also the results from the deconvoluted data for C1s in Table I are in close agreement for silicone-*graft*-PGMA and PGMA. 6.8 atom-% O-C=O carbon and 19.2 atom-% O-C carbon that can be attributed to the epoxy moieties are observed. In the

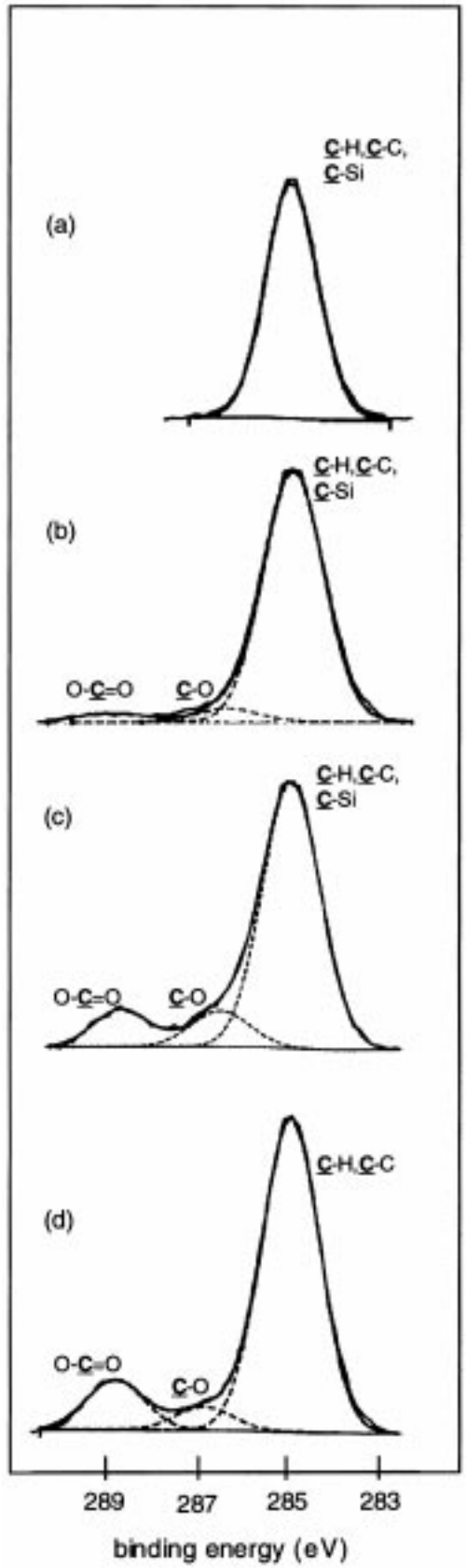

Figure 2 Overlay of XPS (C1s) for (a) untreated silicone; (b) silicone-*graft*-PAAc; (c) silicone-*graft*-PAAc(v); (d) PAAc.

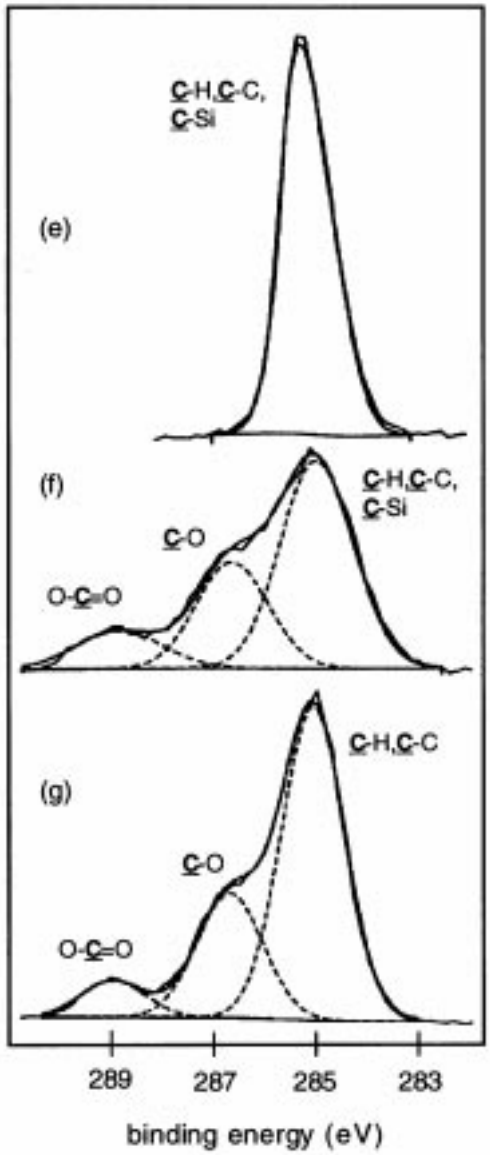

Figure 3 Overlay of XPS (C1s) for (e) untreated silicone; (f) silicone-*graft*-PGMA 1; (g) PGMA.

O1s spectral data (Table I) of (f) two peaks with a ratio of about 4 : 1 at 532.6 and 533.8 eV are observed. The first peak is assigned to Si-O, O-C=O and oxirane oxygen whereas the second peak refers to O-C=O oxygen. Thus, grafting of GMA on silicone leads to a thicker graft layer than grafting of AAc and MAAc. Anyhow, 10.0 atom-% silicon are still detected on the surface. This is in contrast with the results of IR-ATR analysis that points to a surface layer in the range of 0.1 μm thickness. The contradiction is explained by a migration effect in order to minimize surface energy while storing of the sample in air or in vacuum [24].

IR-ATR and XPS work in air and in vacuum, respectively. To characterize the surfaces in contact with water, dynamic contact angle measurements were carried out.

The advancing (Θ_a) and receding (Θ_r) water contact angle of untreated silicone is large $(\Theta_a = 115°; \Theta_r = 85°)$ (Fig. 4) indicating the hydrophobic nature of the material. After argon plasma treatment Θ_a decreases by about 17° giving rise to a change in wettability wherease Θ_r shows a neglegible change. Contact angle hysteresis $(\Theta_a - \Theta_r)$ decreases from 30° to 21°. This points to a slight increase in homogeneity.

The graft-co-polymerization of PMAAc leads to an increase in surface hydrophilicity, as expected for a hydrogel present on the surface. For silicone-*graft*-PAAc this effect is even more pronounced. Silicone-*graft*-PAAc(v) shows a similar Θ_a and a significantly higher

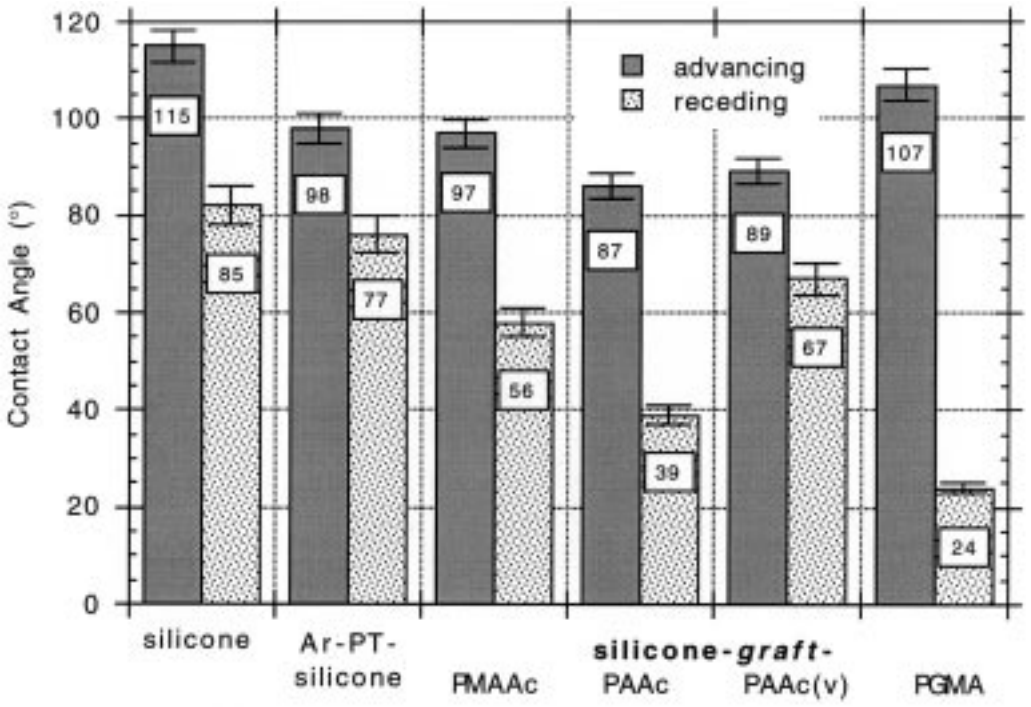

Figure 4 Advancing (Θ_a) and receding (Θ_r) contact angles of water on untreated and surface modified silicone (Wilhelmy-plate method).

Θ_r in comparison with silicone-*graft*-PAAc. The contact angle hysteresis of about 40° for silicone-*graft*-PMAAc and silicone-*graft*-PAAc points to a quite heterogenous surface or to molecular reorganization effects taking place. However, the vapor phase grafted surface seems to be rather homogenous showing a hysteresis of 22°. A very large hysteresis (83°) is measured for silicone-*graft*-PGMA. This may be contributed to a large degree of heterogeneity but also to dynamic swelling effects and molecular rearrangements.

In the aqueous environment, hydrophilic grafts are preferably situated on the outer surface in order to minimize interfacial free energy.

For all modification steps, SEM revealed a uniformly smooth surface. Magnifications up to 4000× did not show any characteristic topology for any of the surfaces except for silicone-*graft*-PGMA. A representative micrograph of the latter is shown in Fig. 5. Hills homogenously spread over the surface are formed. The diameter of the hills is about 0.5 µm. A deeper view into the surface topology is provided by AFM.

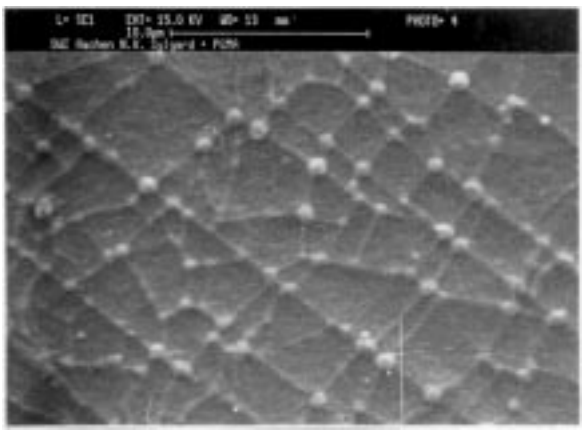

Figure 5 SEM of the surface of silicone-*graft*-PGMA.

AFM allows the analysis of the surface topology in the range of 5 µm. Scanning the silicone surface in contact mode, a surface appears containing pads and beads originating from the molding process (Fig. 6a). After argon plasma treatment, the pads disappear while fissures of about 200 nm width and 30 nm depth are formed (Fig. 6b). Grafting of AAc leads to a filling of the fissures and an even layer of PAAc (Fig. 6c). No significant difference is seen for the different grafting techniques. An analogous result to the one for PAAc is obtained for silicone-*graft*-PMAAc. The thickness of the hydrogel surface was measured and is at about 7 nm. Silicone-*graft*-PGMA (Fig. 6d) shows a much rougher surface. Grooves and fissures are seen but do not necessarily coincide with the ones formed after plasma treatment. Hills on the borders of the fissures might coincide with the structures obtained by SEM.

3.2. Immobilization of hFn onto functionalized silicone

One major aim of this study was to immobilize hFn under retention of its bioactivity as a cell adhesion mediator. Therefore, to characterize the amount of surface-bound protein, a sandwich ELISA was applied. A structure-specific primary antibody was used the epitope of which is the cell-binding domain, the 12 kDa fragment Fn III-10. The secondary antibody was a HRP-linked standard antibody. Therefore, only those protein molecules presenting their cell-binding domain accessible to the antibody are recognized. Fig. 7 shows the results that were obtained from immobilization studies. Values were normalized to hFn adsorbed onto untreated silicone. As can be concluded from Fig. 7, the TCPS used shows only 8% of binding capacity of hFn. Grafting of PAAc or PMAAc also leads to a decrease in immobilized protein amount compared to untreated silicone. This is due to the hydrogel character of the graft polymers as can be seen

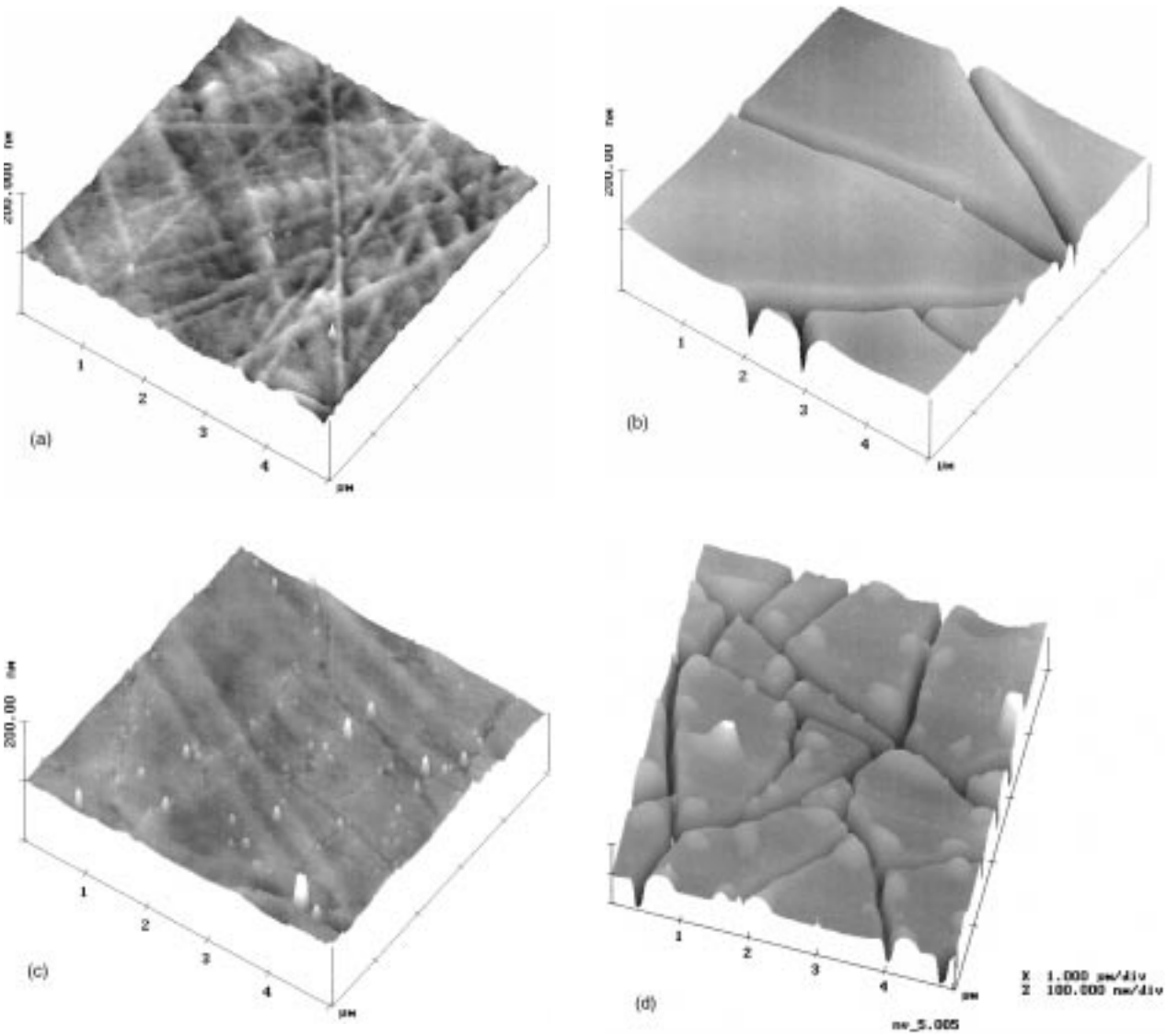

Figure 6 Contact mode AFM images of different surfaces: (a) untreated silicone; (b) Ar-PT-silicone; (c) silicone-*graft*-PAAc; (d) silicone-*graft*-PGMA.

from their high wettability determined by contact angle measurements. In comparison, carboxylic groups of silicone-*graft*-PAAc and silicone-*graft*-PMAAc were reacted with EDC in order to allow subsequent covalent protein immobilization by reaction with protein amino groups under mild reaction condition. Consequently, the binding capacity raised up to the level of untreated silicone, for silicone-*graft*-PAAc (EDC-activated) even 139% were found. This points to a superposition of adsorptive and covalent binding that both contribute to the binding capacity of hFn onto the EDC-activated surfaces.

However, silicone-*graft*-PGMA contains epoxy moieties that need not be further activated for the reaction with amino nucleophiles. hFn was immobilized onto this graft polymer in carbonate buffer of pH 9.6. A highly increased amount of bound hFn was detected (220%). Part of the increase might be contributed to an increase in surface area as assessed by AFM. The surface area difference is about 5% whereas the difference in protein adsorption is 120%. Therefore, the increase of binding capacity for hFn is partly due to covalent bonding between protein and silicone-*graft*-PGMA while the other part derives from adsorptive binding.

3.3. Cytotoxicity

All surfaces did not show toxicity in indirect contact to L929 cells. None of the test materials released any toxic material during 24 h of elution as assessed by vital fluorescence staining, cell morphology, and MTT test.

Viability was tested for different surface modification steps in direct contact. On untreated silicone only vital cells were seen after 24 h. However, cells were globy. Hemalaun staining showed degenerative changes and spindle-shaped cell morphology. Plasma treatment does not lead to a significant improvement of cell growth. However, cell characteristics on samples grafted with AAc, MAAc or GMA were similar to those on the glass control. Cells adhere confluently to the surfaces. Likewise, cells appeared well spread and fibroblasts at different stages of division were often observed. Immobilization of hFn onto the functionalized silicones before contact with cells did not show further improvement of cell growth. However, the effect of hFn immobilization upon the growth of L929 cells depends on the nature of the silicone surface presented. Fig. 8 shows L929 cells after 24 h of incubation onto silicone with adsorbed hFn (a) and

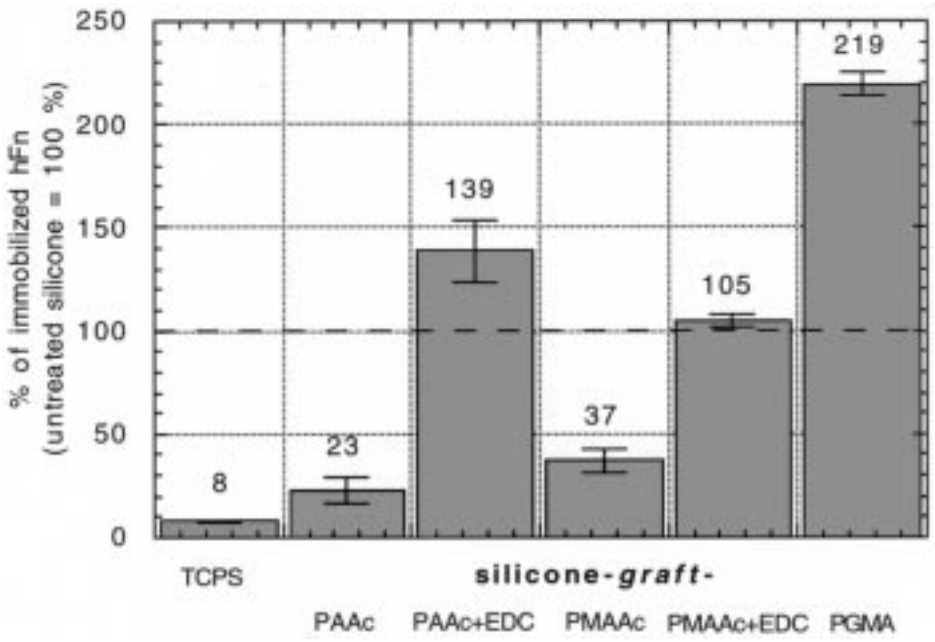

Figure 7 Binding capacity of hFn onto surface modified silicones in percent relative to untreated silicone.

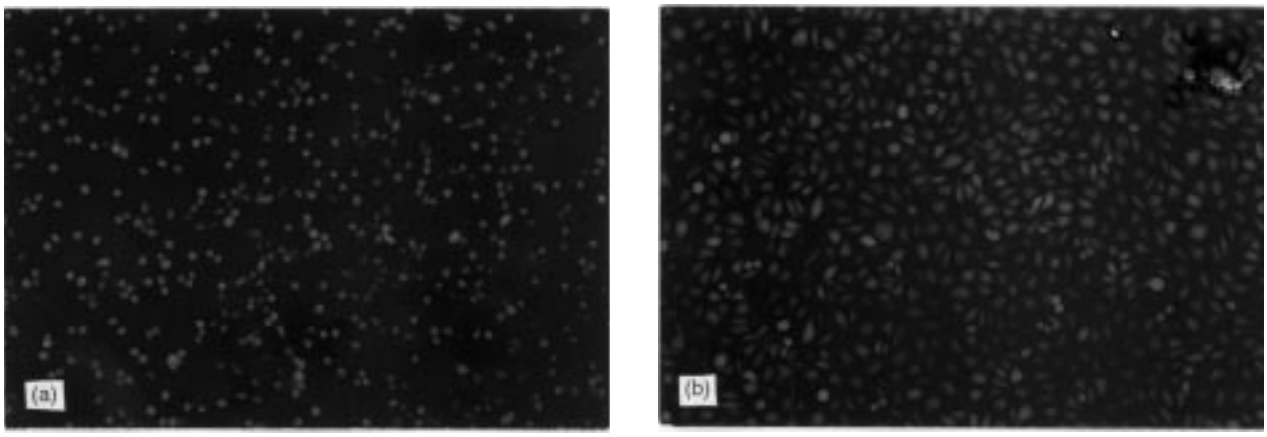

Figure 8 Vital fluorescence staining micrographs of: (a) untreated silicone with adsorbed hFn; (b) silicone-*graft*-PAAC (EDC-activated) with immobilized hFn.

silicone-*graft*-PAAc (EDC-activated) with immobilized hFn (b). A tremendous difference is observed. Preadsorption of hFn does only poorly improve cell growth on silicone, whereas L929 cells grow confluently on a surface containing hFn attached to reactive groups of the grafted layer.

4. Conclusion

The present results show that the described surface modification procedures for silicone rubber provide reactive acid and epoxy moieties within a hydrogel layer on the silicone surface. Grafting of GMA leads to a thicker grafted layer compared to grafting of AAc and MAAc. There are hints for reorganization phenomena working on surface modified silicones during storage in air or vacuum that have to be further investigated. Via the reactive groups, hFn is bound covalently onto the surface of silicone. ELISA studies showed highest amounts of active hFn for silicone-*graft*-PGMA. Cell culture studies revealed clear differences regarding the action of the cell adhesion mediator onto L929 cells depending on whether it is adsorbed-only or covalently attached to a hydrophilic graft-co-polymer on the surface. Cytocompatibility is highly increased for the latter. The properties of the described functionalized silicone rubber open potential applications of these materials as ophthalmological implants.

Acknowledgments

Vapor phase graft-co-polymerization was done at the Institute of Physics at the Technical University of Chemnitz-Zwickau. The authors gratefully acknowledge support by the Interdisciplinary Center for Clinical Research ''BIOMAT''.

References

1. B. ARKLES, *CHEMTECH* **13** (1983) 542.
2. M. REIM, *Ophthalmology* **89** (1992) 109.
3. L. REINBACHER, *Ärztlicher Praxis* **96** (1995) 5.
4. S. A. VISSER, R. W. HERGENROTHER and S. L. COOPER in ''Biomaterials Science: An Introduction to Materials in Medicine'', edited by B. D. Ratner, A. S. Hoffman, F. J. Schoen and J. E. Lemons (Academic Press, New York, 1998) p. 59.
5. S. S. BACON, C. ASTIN and J. DART, *Cornea* **13** (1994) 422.

6. G. KOERNER, M. SCHULZE and J. WEIS (editors) in ''Silicones: Chemistry and Technology'' (Vullkan Publishing, Essen, 1991).
7. S.-H. CHANG, US Patent, WO 91/04288, 1991.
8. H.-J. HETTLICH, F. OTTERBACH and C. MITTERMAYER, *Biomaterials* **12** (1991) 521.
9. T. OKADA and Y. IKADA, *J. Biomed. Mater. Res.* **26** (1992) 1569.
10. G. H. HSIUE, S.-D. LEE, C.-C. WANG and P. CHANG, *J. Biomater. Sci. Polymer Edn.* **5** (1993) 205.
11. A. S. HOFFMAN in ''Biomaterials Science: An Introduction to Materials in Medicine'', edited by B. D. Ratner, A. S. Hoffman, F. J. Schoen and J. E. Lemons (Academic Press, New York, 1998), p. 128.
12. G.-H. HSIUE, S.-D. LEE, C.-C. WANG, M. HSIUE and P. CHANG, *Biomaterials* **15** (1994) 163.
13. T. A. HORBETT, in ''Protein Adsorption to Hydrogels'' (Vol. 1, CRC Press, 1986).
14. S. SANO, K. KATO and Y. IKADA, *Biomaterials* **14** (1993) 817.
15. L. J. GOGUÉ, N. MERMILLIOD and A. GANDINI, *J. Appl. Polym. Sci.* **56** (1995) 33.
16. X. COQUERET, A. LABLACHE-COMBIER and C. LOUCHEUX, *Eur. Polym. J.* **24** (1988) 1137.
17. D. F. MOSHER, *Ann. Rev. Med.* **35** (1984) 561.
18. J. G. STEELE, B. A. DALTON, G. JOHNSON and P. A. UNDERWOOD, *Biomaterials* **16** (1995) 1057.
19. A. S. HOFFMAN, *Artificial Organs* **16** (1992) 43.
20. J. M. LEE, H. H. L. EDWARDS, C. A. PEREIRA and S. I. SAMII, *J. Mater. Sci.: Mater. Med.* **7** (1996) 531.
21. C. J. CLIFFORD and S. DOWNES, *ibid.*, **7** (1996) 637.
22. J. G. A. TERLINGEN, H. F. C. GERRITSEN, A. S. HOFFMAN and J. FEIJEN, *J. Appl. Polym. Sci.* **57** (1995) 969.
23. B. RATNER and D. G. CASTNER, *Coll. Surf. B: Biointerfaces* **2** (1994) 333.
24. M. J. OWEN, T. M. GENTLE, T. ORBECK and D. E. WILLIAMSIN, in ''Polymer Surface Dynamics'', edited by J. Andrade (Plenum Press, New York, 1988), p. 101.